Kinetics and Catalysis, Vol. 43, No. 1, 2002, pp. 139–145. Translated from Kinetika i Kataliz, Vol. 43, No. 1, 2002, pp. 150–156.

The Role of Surfactants in the Formation of Highly Dispersed Iron–Zirconium Oxide Composites with Uniform Pores

A. S. Ivanova, M. A. Fedotov, G. S. Litvak, S. N. Trukhan, and V. P. Ivanov

Boreskov Institute of Catalysis, Siberian Division, Russian Academy of Sciences, Novosibirsk, 630090 Russia

Received May 12, 2000

Abstract—The effects of the nature and concentration of surfactants and the preparation conditions on the genesis of iron–zirconium composites with a $[Fe^{3+}]/[Zr^{4+}]$ ratio of 0.123 were studied. The effect of surfactants on the physicochemical properties of precipitates is determined by the conditions of synthesis. The amount of surfactants retained by the precipitate at pH ~3 is about an order of magnitude greater than at pH ~9. The thermolysis of samples synthesized at acidic pH is accompanied by the dehydration and dehydroxylation of iron–zirconium composites as well as by the decomposition and destruction of surfactants. In the latter processes, compounds or their fragments capable of reducing some phases are removed in a stepped-up manner. The specific surface area of oxide systems formed in this way is at most 100–150 m^2/g. In the pH range corresponding to the complete precipitation of the components, highly dispersed single-phase and uniformly porous composites are formed. The choice of a surfactant, its fraction, and preparation conditions enables the preparation of oxides with specific surface areas of 100–400 m^2/g. The average pore diameter of the samples ranges from 3.0 to 27.0 nm, and the total pore volume ranges from 0.20 to 0.38 cm^3/g.

INTRODUCTION

Sol–gel synthesis in the presence of surfactants is a possible method for controlling a particle size in hydroxide and oxide systems [1]. This is due to the fact that the addition of a surfactant is accompanied by a significant change in the properties of supersaturated solutions. For instance, the surface tension of an intermicellar liquid may change and affect the size, morphology, and the spatial orientation of prepared crystals.

The goal of this work was to study the effect of surfactants and their fractions on the phase composition, dispersion, and pore structure of the iron–zirconium system.

EXPERIMENTAL

The Fe–Zr–O system with a molar ratio $[Fe^{3+}]/[Zr^{4+}]$ of 0.123 was chosen for the study. Samples were prepared by the addition of a base (2 mol/l KOH) to a solution containing iron and zirconyl nitrates and a certain amount of the surfactant. Then, the suspension was allowed to stay at 20°C and an elevated temperature for different times (τ). The suspensions were filtered, and the precipitates were washed with distilled water until the nitrates in the filtrate disappeared. The samples were dried in air and then in a dry box at 110°C for 12 h and calcined in a dry air flow at 400–700°C for 4 h. The solutions of glycerol, polyvinyl alcohol, carboxymethylcellulose, sodium salt of ethylenediaminetetraacetic acid (NaEDTA), and stearic acid were used as surfactants.

The concentrations of main components in the samples were determined by atomic absorption spectroscopy [2]. The state of the components in the liquid phase was studied by NMR on different nuclei as described in [3]. In solutions containing paramagnetic (Fe^{3+}) ions, the concentration of the mononuclear species Fe^{3+} + $(FeOH)^{2+}$ can be estimated from the ^2D NMR line width of water. The effect of polynuclear paramagnetic species on the line width is not strong because of a decrease in the effective magnetic moment due to spin–spin interaction. The formation of colloidal particles causes a sharp broadening of the lines in the ^{14}N NMR spectra. This makes it possible to estimate the presence of colloidal particles in a solution.

Thermal analysis was carried out using a Derivatograph-Q-1500 D at 20–1000°C in air at a heating rate of 10°/min. A sample loading was 0.2 g, and the accuracy in the determination of weight loss was ±0.5%. Studies by secondary ion mass spectrometry were performed using an MS-7201 secondary ion mass spectrometer automated by a PC and KAMAK interface. The spectral region with masses from 45 to 135 was periodically scanned during recording the secondary emission spectra. The recording period for each cycle was 150 s. Samples were previously deposited on a support covered with indium of high purity to avoid their charging. The Ar^+ ions with an energy of 4 keV were used as a primary beam. The density of current was 20 $\mu A/cm^2$. The textural characteristics of the samples were calculated from the isotherms of low-temperature (–196°C) nitrogen adsorption measured using an ASAP-2400 Micromeritics setup according to a standard procedure [4] with the use of the desorption branch.

0023-1584/02/4301-0139$27.00

Table 1. The ^2D and ^{14}N NMR data for iron–zirconium samples with the ratio [Fe]/[Zr] = 0.123 and various surfactants

Surfactant		pH	$\kappa = [OH]/[\Sigma M]$	$\delta(^2D)$, ppm	$\delta(^{14}N)$, ppm	$\delta(^2D) - \delta(^{14}N)$, ppm
type	amount, wt %					
Without surfactant	0	0	0	1.50 (98)	−1.3 (38)	2.80
		0.75	0.66	1.00 (78)	−0.5 (39)	1.50
		1.00	1.05	0.95 (84)	−0.3 (42)	1.25
		1.50	1.30	0.80 (79)	−0.3 (40)	1.10
		2.00	1.77	0.24 (67)	0.5 (132)	−0.26
Glycerol	1	0	0	1.6 (98)	−1.32 (47)	2.9
		1.00	1.36	0.9 (63)	−0.26 (46)	1.2
		2.00	2.04	0.2 (50)	0.79 (137)	−0.6
		2.50	2.32	−0.2 (38)	1.06 (220)	−1.3
Polyvinyl alcohol	1	0.05	0	1.95 (94)	−1.32 (47)	3.27
		0.50	0.54	1.39 (73)	−0.53 (53)	1.92
		1.00	1.05	1.01 (68)	−0.26 (48)	1.33
		1.50	1.37	0.85 (58)	0.26 (51)	0.57
		2.00	1.80	0.20 (44)	1.06 (100)	−0.86
Carboxymethylcellulose	1	−0.92	0	2.2 (113)	−1.9 (42)	4.1
		0.50	0.94	1.6 (82)	−0.9 (46)	2.5
		0.75	1.25	1.4 (73)	−0.8 (42)	2.2
		1.25	1.80	1.2 (67)	−0.5 (48)	1.7
		1.75	2.27	0.5 (49)	0.5 (69)	0

Note: The line width in the NMR spectrum, Hz, is shown in parenthesis. The chemical shifts and line widths in the NMR spectrum for the D_2O and NO_3^- standards are 0 (30).

RESULTS AND DISCUSSION

It is known that, when bases are added to the solutions of salts, hydrolysis and polycondensation sometimes occur to produce polynuclear hydroxy complexes. These complexes, in turn, affect the properties of precipitates.

Table 1 presents NMR data on hydrolysis in the surfactant-containing solutions of iron and zirconyl nitrates. The paramagnetic shift for water ($\delta^2D - \delta^{14}N$) was calculated using $\delta^{14}N$ of the NO_3^- ion as a correction for the bulk magnetic susceptibility. The paramagnetic shift of the NO_3^- ion in these solutions was less than 0.3 ppm. It is seen in Table 1 that a surfactant affects the κ value: $\kappa = [OH]/[\Sigma M]$ where $[\Sigma M]$ is the overall concentration of iron and zirconyl ions that lets colloidal particles appear. In the absence of the surfactant, the colloidal particles are formed at $\kappa = 1.77$ and the introduction of 1% of surfactant is accompanied by an increase in κ, indicating the deceleration of the colloidal particle formation. According to the data of Table 1 and [5], the rate of colloidal particle formation decreases in the following surfactant series: polyvinyl alcohol < glycerol < carboxymethylcellulose.

Figure 1 shows potentiometric curves. As expected, their shape is determined by the surfactant nature. However, precipitation in all cases is completed in the equivalent point (pH 9). At lower pH, hydrolysis and polycondensation occur and the influence of a surfactant is more pronounced in this range. Therefore, we studied the properties of iron–zirconium systems as a function of the surfactant nature and the conditions of synthesis.

According to the thermal analysis data (Fig. 2), endothermic and exothermic effects are seen on the DTA curves, and the appearance and positions of the effects depend on the surfactant nature and the conditions of synthesis. The shapes of DTA curves for samples prepared under the same conditions (pH 9, $\tau = 24$ h) with different surfactants (Fig. 2, curves *2*–*5*) differ insignificantly. Figure 2 (curve *3*') shows a typical differential thermal gravimetric (DTG) curve. When the surfactant is introduced, the low-intensity exothermic effects appear in a temperature range of 290–340°C, which is probably due to the surfactant decomposition.

The temperature of the exothermic effect due to the crystallization of a solid solution on the basis of cubic zirconium dioxide increases to 615–625°C. A small endothermic effect at 850–865°C is also observed. Thermolysis occurs differently in the case of samples synthesized at pH 3 (Fig. 2, curves *6* and *7*). For the sample prepared in the presence of NaEDTA, stepped decomposition first occurs at 240, 305, and 410°C (Fig. 2, curve *6*'). Then, the exothermic effect is seen at 450°C, and a small endothermic peak accompanied by a weight change is seen near 760°C. A similar behavior was found for the sample prepared in the presence of carboxymethylcellulose (Fig. 2, curve *7*). A broad endothermic effect with a minimum at 160°C on the DTA curve is accompanied by the stepped removal of the products at 140, 215, and 245°C and the number of endothermic effects increases: they are seen at 310, 350, 405, 455, and 475°C. The temperature of exothermic effect shifts to higher temperatures and equals 505°C; an implicit exothermal peak is seen at 595°C. However, the oxide structure is formed at temperatures below 835°C, as can be seen from a small smooth weight loss below the above temperatures.

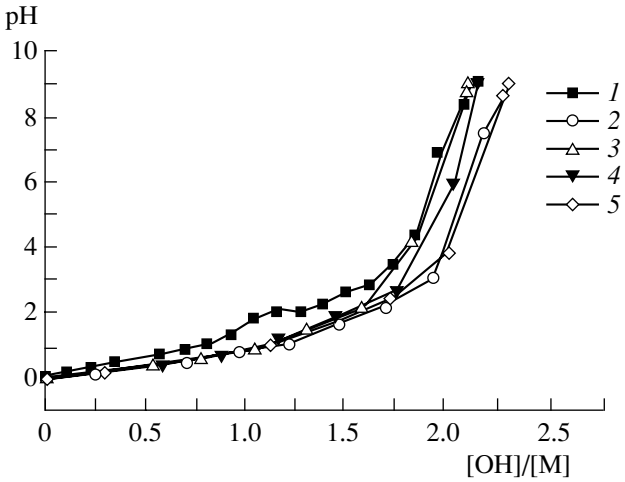

Fig. 1. Curves of titration of mixed solutions of iron and zirconyl nitrates with the ratio $[Fe^{3+}]/[Zr^{4+}] = 0.123$ (*1*) without a surfactant and containing the following surfactants: (*2*) glycerol; (*3*) polyvinyl alcohol; (*4*) carboxymethylcellulose; and (*5*) NaEDTA.

These differences are confirmed by data from the mass spectrometric studies of thermal desorption [5] from the samples prepared in the presence of NaEDTA at various pH. The examination of spectra presented in [5] shows that surfactant decomposition occurs in steps in several temperature ranges with maxima at 250, 350, 450, and higher than 500°C; this agrees with the thermal analysis data (Fig. 2, curves *6* and *6*'). It is difficult to identify the compounds that desorb to the gas phase because different compounds or their fragments give peaks with the same masses in the mass spectra. Nevertheless, some assumptions can be made. The compounds containing the CH_xNH_x groups probably desorb at 250°C. This follows from the fact that the low-temperature tails with masses 30 and 44 are present in the spectra [6]. At 350°C, the compounds containing the CH_2 (*m/e* = 14), OH (*m/e* = 17), and CO (*m/e* = 28) groups desorb to the gas phase. Masses 28, 30, 31, 44, and 45 found at 450°C probably indicate the presence of CO, NO, CH_3NH_2 (methylamine), CH_3CHO (acetaldehyde), and $(CH_3)_2NH$ (dimethylamine) in the gas phase. A further increase in the desorption temperature to 500–600°C favors the decomposition of other organic compounds remaining on the surface to form N_2, CO, and CO_2.

A typical secondary ion mass spectrum for calcined samples is shown in Fig. 3. The following peaks are present in the spectra of all samples:

m/e	Ion (concentration, %)
54, 56	$^{54}Fe^+$(6), $^{56}Fe^+$(92)
90, 91, 92, 94, 96	$^{90}Zr^+$(51), $^{91}Zr^+$(11), $^{92}Zr^+$(17), $^{94}Zr^+$(17), $^{96}Zr^+$(3)
106–108, 110, 112	ZrO
113, 115	^{113}In, ^{115}In (sample support)
73	$^{56}FeOH^+$
109, 111	$^{92}ZrOH^+$, $^{94}ZrOH^+$
123	$^{90}ZrO_2H^+$

The presence of peaks with *m/e* 73, 109, and 123 in the spectra (peak with *m/e* 122 for $^{90}ZrO_2^+$ is absent) indicates that hydroxy groups are present in the bulk of oxides, especially in the samples calcined at 400°C. The peaks with *m/e* 78, 80, and 95, which correspond to the $^{39}K^{39}K^+$, $^{39}K^{41}K^+$, and $^{56}Fe^{39}K^+$ dimers, were found for the samples synthesized at pH 3.

The ratios of ionic currents in $^{56}Fe^+/^{90}Zr^+$ and $^{90}ZrO^+/^{90}Zr^+$ on the surface (~20 Å) and in the bulk (when the stationary intensity of signals was reached,

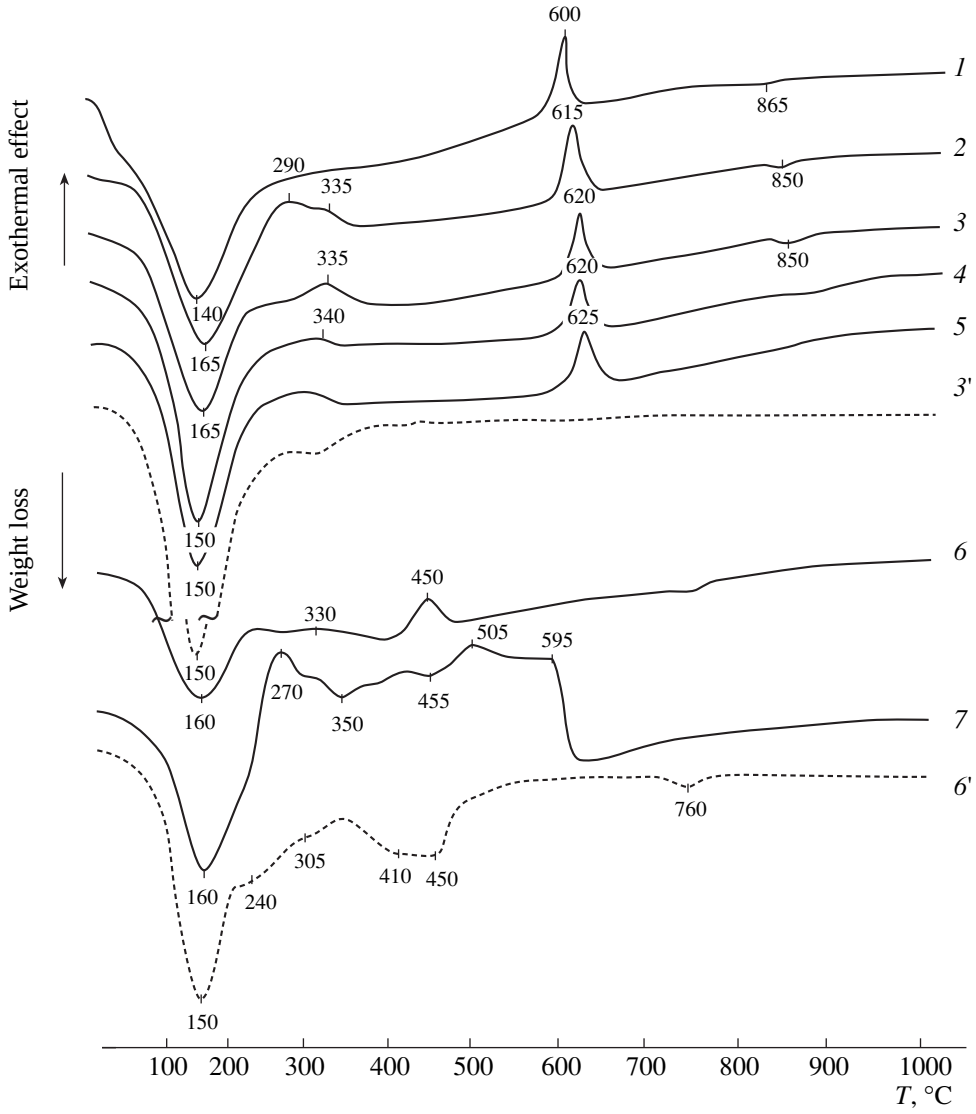

Fig. 2. Curves of DTA (*1–7*) and DTG (*3′*, *6′*) for iron–zirconium samples prepared at (*1–5*) pH 9 and (*6*, *7*) pH 3 with differing surfactants: (*2*) glycerol, (*3*) polyvinyl alcohol, (*4*) carboxymethylcellulose, (*5*, *6*) NaEDTA, and (*7*) stearic acid.

the depth was ~500 Å) are presented in Table 2. As can be seen, an increase in the calcination temperature for the samples prepared at different pH results in a decrease in the $^{56}Fe^+/^{90}Zr^+$ ratio by 1.5 times. The differences in the $^{90}ZrO^+/^{90}Zr^+$ ratio for various samples are also observed. These effects can be explained by phase transformations occurring in the samples. The elemental environment of an atom of each kind and the bond lengths can vary with an increase in the temperature, leading to a change in the ionization probability of any component [7]. Then, it is known [8] that the MO^+/M^+ ratio reached upon the sputtering of oxides is nearly proportional to the dissociation energy of the metal–oxygen bond, which can also change with a change in the phase composition. The $^{90}ZrO^+/^{90}Zr^+$ values for different modifications of ZrO_2 were measured in separate experiments. This ratio proved to be 0.6–0.9 for cubic and tetragonal modifications and 0.3–0.4 for monoclinic modification under our conditions. Therefore, we conclude that, in the samples synthesized at pH 9, cubic or tetragonal zirconium dioxides are formed; in the samples prepared at pH 3 and calcined at 400°C, the same phases are formed as in the above case, and after calcination at 700°C, the monoclinic zirconium dioxide or other phases are formed. These findings further confirm that the phase composition of samples depends on the precipitation conditions [5]. A twofold decrease in the $^{56}Fe^+/^{90}Zr^+$ value for the samples prepared at pH 3 compared to those synthesized at pH 9 is probably due to the presence of potassium bound to iron (the molecular ion FeK^+ was detected by spectroscopy) because electropositive elements decrease the ionization probability for the neighboring elements of a matrix during their emission [9]. As can be seen from

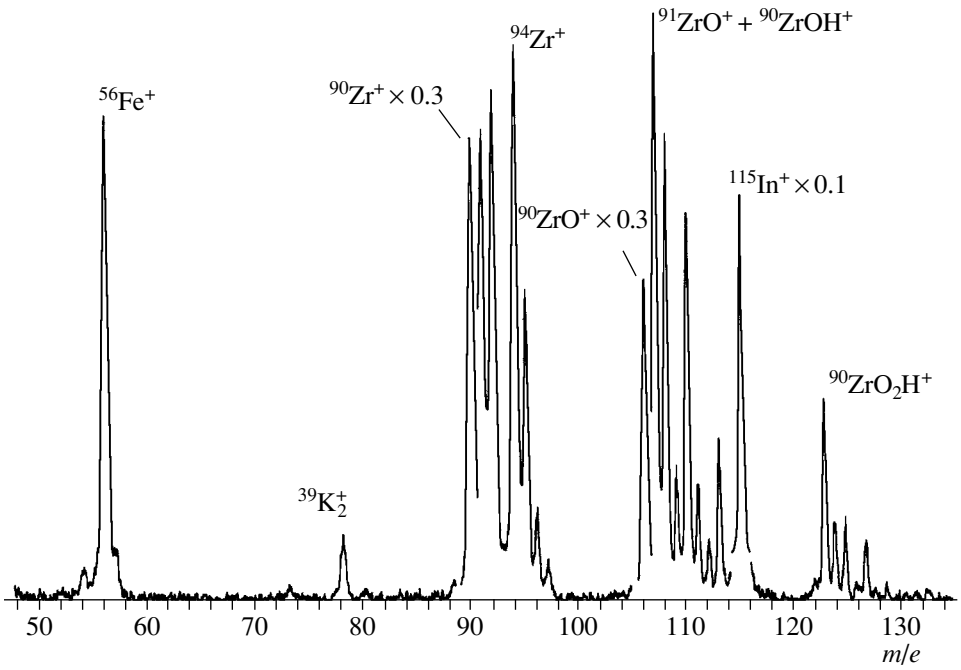

Fig. 3. Secondary ion mass spectrum for the sample synthesized in the presence of NaEDTA at pH 3 and calcined at 400°C. The etching depth is 50 nm.

Table 2, the ratio of signals $^{56}Fe^+/^{90}Zr^+$ is ~5 times higher on the surface than in the bulk. Such a difference is most probably due to the enrichment of the surface with iron, because only a twofold decrease in this ratio can be explained by the effect of the predominant sputtering of ^{56}Fe atoms compared to ^{90}Zr atoms [10]. Note that the $^{56}Fe^{39}K^+/^{90}Zr^+$ and $^{56}Fe^+/^{90}Zr^+$ ratios are lower on the surface than in the bulk.

Thus, our study confirmed that the phase compositions of samples synthesized in the presence of the same surfactant but at different pH of precipitation are different. On the one hand, this is due to the presence (pH 3) or absence (pH 9) of interaction between the surfactant and iron or zirconium polyhydroxy complexes at the stage of precipitation. On the other hand, this can be a result of the decomposition and destruction of a surfactant during thermal treatment. These processes occur along with the dehydration and dehydroxylation of iron–zirconium composites, and the compounds or their fragments are capable of reducing the corresponding phases.

The introduction of the surfactant into iron–zirconium composites and the phase transformations occurring in them change their textural characteristics [5]. The synthesis of iron–zirconium samples performed by the addition of a base to a solution of corresponding salts until reaching pH 9 in the presence of surfactant allows one to produce highly dispersed composites differing in pore structures at 110–700°C [5].

According to low-temperature nitrogen adsorption, the adsorption isotherms for the samples synthesized at pH 9, which contained 1 wt % of a surfactant, have the same shape irrespective of the surfactant nature [5]. However, the absolute values of the textural characteristics of samples are determined by the real conditions of their preparation. It is seen (Table 3) that the specific surface areas and pore volumes of the samples prepared under the same conditions and containing 1 wt % polyvinyl alcohol increase with aging time. The micropore

Table 2. The ionic current ratios for the corresponding components on the surface and in the bulk of iron–zirconium samples

pH	Calcination temperature, °C	$^{56}Fe^+/^{90}Zr^+$		$^{90}ZrO^+/^{90}Zr^+$	
		surface	bulk	surface	bulk
9	400	~3	0.6	0.50	0.50
	700	~2	0.4	0.58	0.58
3	400	~1.5	0.3	0.69	0.69
	700	~1	0.2	0.44	0.44

Table 3. Textural characteristics of the iron--zirconium samples

Preparation conditions			Surfactant		Calcination temperature, °C	N_2 adsorption				
pH	T, °C	τ, h	polyvinyl alcohol	content, wt %		S_{sp}, m^2/g	V_p, cm^3/g (±3%)	V_{micro}, cm^3/g (±50%)	structure type*	d_{av}, nm (±5%)
9	110	2	polyvinyl alcohol	1.0	400	240	0.19	0.0120	mono-	3.2
the same	the same	24	the same	the same	400	250	0.26	0.0105	mono-	4.8
″	″	48	″	″	400	321	0.31	0.0161	mono-	3.9
″	″	120	″	″	400	326	0.35	0.0104	mono-	4.3
″	″	120	″	″	700	110	0.20	0.0013	mono-	7.6
″	″	24	NaEDTA	1.0	400	290	0.26	0.0208	mono-	3.6
″	″	24	polyvinyl alcohol	6.0	400	220	0.20	0.0081	bi-	3.8
″	″	24	stearic acid	25.0	400	170	0.28	0.0036	poly-	6.6
″	″	24	NaEDTA	40.0	400	2.3	0.0026	0.0002	poly-	4.4
3	″	24	NaEDTA	1.0	400	10	0.013	0.0021	bi-	4.7
the same	″	24	stearic acid	5.0	400	31	0.072	0.0018	bi-	9.2
″	″	24	″	25.0	400	130	0.38	0.0018	poly-	11.7
″	″	24	″	25.0	700	30	0.20	0.0011	poly-	27.0

* The nature of the size distribution of particles: mono-, bi-, and poly- are monodisperse, bidisperse, and polydisperse distributions.

volume remains unchanged with reasonable accuracy. The average pore diameter changes slightly and equals (4.0 ± 0.8) nm for the above samples. A replacement of polyvinyl alcohol by NaEDTA favors only an increase in the fraction of micropores (Table 3), whereas the other characteristics are comparable to those for the corresponding sample containing polyvinyl alcohol.

When the temperature of sample treatment is increased to 700°C, the redistribution of pore sizes does not occur (Table 3). Only a decrease in the absolute values of the specific surface area, pore volume, and the fraction of micropores was found. The samples also had the monomesoporous structure, and only the average pore size increased.

Other conditions being the same, an increase in the fraction of the surfactant in the samples leads to the redistribution of pore sizes (Table 3). The efficiency of the surfactant is determined by its amount. As can be seen, the addition of 6 wt % polyvinyl alcohol favors the formation of a biporous structure and slightly affects other textural parameters. An increase in the surfactant fraction (stearic acid) to 25 wt % causes a decrease in the specific surface area, an increase in the pore volume, and the polydisperse pore size distribution. The textural changes are primarily observed upon the addition of 40 wt % NaEDTA in the iron–zirconium composite. The specific surface area of the sample is 2.3 m^2/g, the pore volume is 0.0026 cm^3/g, and the pore size distribution is polydisperse. These changes in the specific surface area and pore structure are likely due to the fact that the surfactant introduced into the sample in the increased amount does not decompose completely at the temperature of 400°C; it blocks the pore space, and the surface of particles becomes inaccessible for adsorbate molecules.

A similar genesis of the texture is observed in the samples prepared at low pH in the presence of a surfactant (Table 3). In this case, the bimodal or polydisperse pore distributions are also observed. At a NaEDTA concentration of 1 wt %, the specific surface area only reaches 10 m^2/g and the pore volume is 0.013 cm^3/g. A replacement of NaEDTA by stearic acid and an increase in its fraction to 5 wt % favors an increase in all textural parameters, but the pore volume becomes 0.072 cm^3/g. However, the texture of the samples prepared at low pH changes due to the fact that not only the hydroxide species but also the significant amount of low-temperature species are formed, which favor the formation of coarsely dispersed compositions [11]. Other conditions being the same, a further increase in the amount of stearic acid to 25 wt % allows the preparation of a sample with a large surface area and a pore volume of 0.38 cm^3/g. The average pore diameter increases to 11.7 nm. An increase in the temperature of treatment to 700°C does not affect the pore size distribution as in the case of the samples prepared at pH 9. Only the specific surface area and pore volume decrease, while the average pore diameter increases (Table 3).

The above findings suggest that it is possible to control the textural characteristics of iron–zirconium composites over a wide range by choosing appropriate conditions for synthesis and surfactant. As a result, mono-, bi-, and polymesoporous systems with relatively large overall pore volumes are formed.

REFERENCES

1. Il'icheva, A.A., Olenin, A.Yu., Podzorova, L.I., Shevchenko, V.Ya., Lazarev, V.B., and Izotov, A.D., *Neorg. Mater.*, 1996, vol. 32, no. 7, p. 833.
2. Price, W.J., *Analytical Atomic-Absorbtion Spectroscopy*, New York: Heyden & Son, 1976.
3. Ivanova, A.S., Fedotov, M.A., Litvak, G.S., and Moroz, E.M., *Neorg. Mater.*, 2000, vol. 36, no. 4, p. 440.
4. Broekhoff, J.C.P. and de Boer, J.H., *J. Catal.*, 1968, vol. 10, no. 4, p. 368.
5. Ivanova, A.S., *Kinet. Katal.*, 2001, vol. 42, no. 3, p. 394.
6. Sidel'nikov, V.N., Gur'yanova, L.V., Utkin, V.A., and Malakhov, V.V., *Katalog sokrashchennykh mass-spektrov* (Catalog of Short Mass Spectra), Kolchin, A.M., Ed., Novosibirsk: Nauka, 1981.
7. Yu, M.L., *Nucl. Instr. Methods Phys. Res., Sect. B*, 1987, vol. 18, no. 3, p. 542.
8. Wittmaack, K., *Surf. Sci.*, 1979, vol. 89, nos. 1–3, p. 668.
9. Verner, G., *Electron and Ion Spectroscopy of Solids*, Firmans, L., Vennik, J., and Dekeyser, V., Eds., New York: Plenum, 1973.
10. Kelly, R., *Surf. Sci.*, 1980, vol. 100, no. 1, p. 85.
11. Gavrilov, V.Yu., *Kinet. Katal.*, 2000, vol. 41, no. 5, p. 786.